Scanning Microscopy Vol. 12, No. 4, 1998 (Pages 653-665) 0891-7035/98$5.00+.25
Scanning Microscopy International, Chicago (AMF O'Hare), IL 60666 USA

# STEREOSCOPIC IMAGES OF HUMAN CATARACTOUS LENS FIBERS OBTAINED WITH FIELD EMISSION SCANNING ELECTRON MICROSCOPY

W.L. Jongebloed[1*], J.J.L. van der Want[1], J.G.F. Worst[2] and D. Kalicharan[1]

[1]Laboratory for Cell Biology and Electron Microscopy, University of Groningen, The Netherlands
[2]Department of Ophthalmology, Academic Hospital, Groningen and Refajas Hospital, Stadskanaal, The Netherlands

(Received for publication May 11, 1996 and in revised form February 17, 1997)

**Abstract**

Segments of healthy human lenses and lenses with an anterior cortex cataract, prefixed in glutaraldehyde and subsequently postfixed in a mixture of tannic acid - arginine - osmium tetroxide, were examined by stereo-scopic imaging at 2 kV in a field emission scanning electron microscope. The degeneration process of the lens fibers was identified by the presence of spherical bodies or vacuoles in the cytoplasm of the lens epithelial cells, porosity and granulation of the lens fiber membrane and opening (distortion) of the lens fiber interdigitation system. The spherical bodies, containing either a viscous or a low density material, escaped from the cytoplasm penetrating the porous lens cell membrane at several places; this could in particular be observed at the intercellular space between the lens fibers. The stereoscopic pairs of images gave a realistic three-dimensional impression of the ongoing structural alterations during the degeneration process, especially the formation of globular vacuoles protruding from the lens epithelial cytoplasm and their subsequent escape.

**Key Words:** Lens epithelial cells, cataract, spherical bodies, interdigitation system, field emission scanning electron microscopy, stereoscopic images, tannic acid/arginine/osmium tetroxide non coating fixation.

*Address for correspondence:
W.L. Jongebloed
Laboratory for Cell Biology and Electron Microscopy
University of Groningen
Oostersingel 69/2
9713 EZ Groningen
The Netherlands

Telephone Number +31-33-503632501
Fax Number +31-33-503632515
E-mail: w.l.jongebloed@med.rug.nl

## Introduction

### Morphology of the healthy lens

The biconvex human eye lens has an elliptical shape and an average diameter of 4 mm. Its transparency is mainly due to its shape and the arrangement, internal structure and the biochemistry of the lens constituents, epithelial cells and capsule. The lens is surrounded by a transparent elastic capsule; directly beneath the capsule a single layer of cuboidal lens epithelium is found at the anterior, intermediate and equatorial zone (Maisel *et al.*, 1981). At the equator these lens epithelial cells can divide and form highly elongated lens cells with a ribbon-like appearance (which therefore are called lens fibers) growing in the anterior and posterior direction. The newly formed lens cells at the cortex may be 10-12 μm long and 1-2 μm thick; at areas where lens cells converge and meet, sutures are formed (Kessel and Kardon, 1979). In superficial layers of the cortex, interlocking interdigitations are found at the edges along the length of the cells, and at the end of the elongated hexagonal shaped lens cells, the long and short sides of the lens fibers or the broad and narrow faces (Kuszak and Rae, 1982).

There are two types of interlocking devices or lateral interdigitations. The first, generally referred to as ball, emanates from the angle formed by two narrow faces. It consists of a ball-shaped structure on top of a narrow stalk and occurs along the length of the lens fiber. This lateral interdigitation fits into a complementary shaped socket formed at the confluence of broad and narrow faces between opposed lens fibers in successive growth shells. The second type of interlocking device is generally referred to as a flap, and emanates from the angle formed by a broad and narrow face and also occurs along the length of the fibers alternating with the sockets of the balls and sockets mentioned above. This tongue- or flap-shaped outpocketing fits into a complementary shaped imprint formed on the narrow face of opposed lens fibers in successive growth shells. The lateral interdigitation system and the relatively small amount of interstitial fluid in the lens contributes to the transparency of the lens, because the fluid produces only a small change in the refractive index between cells (Hogan *et al.*, 1971). As additional lens cells are formed, older cells may loose their

nuclei and become displaced to deeper parts of the cortex of the lens, surrounding the embryonic nucleus formed initially (Vrensen *et al.*, 1992). The undulating membranes as shown in ultrathin sections in the transmission electron microscope (TEM), corresponding with the grooves and ridges in scanning electron microscope (SEM) images, are found in the deep cortical lens fibers; no gap junctions are seen here, in contrast to the situation in more superficial lens fibers. These communicating junctions have been demonstrated in freeze-fracture/ freeze-etch replicas in TEM (Vrensen *et al.*, 1992). The complex edge protrusions are seen in stereoscopic pairs of SEM images of fractured lens fibers (Willekens and Vrensen, 1982; Kuszak *et al*., 1988). The difference between superficial and deep cortical fibers is not only of an ultrastructural nature, but is also reflected in a different biochemistry of integral membrane proteins and cholesterol. Lens epithelial cells can grow as individual cells on the posterior lens capsule and can form monolayers with a basal lamina (Fagerholm and Philipson, 1977). Fibroblasts and melanocytes adhere to the capsule and proliferate, while epithelial cells can differentiate to fibroblast-like cells causing wrinkling of the posterior capsule and subsequent vision disturbance (Duke-Elder, 1969).

**Morphology of the cataractous lens**

Cataracts are clinically described as a significant decrease of vision due to an irreversible increase in absorption or scattering of light by the lens (Kappelhof *et al.*, 1986; Brown *et al*., 1986; Vrensen and Willekens, 1989). In the western countries cataract formation results mostly from aging or diabetes. Several hypotheses have been postulated about the high prevalence of cataract formation in certain regions. It has been suggested that especially in the non-privileged countries of Asia and Africa racial differences, high mineral intake, heavy yoghurt consumption, ultraviolet (UV) radiation from sunlight and malnutrition could generate cataract formation (Kobayashi and Susuki, 1975; Harding, 1980). Lens fiber compounds, such as glucose and galactose can be reduced to sorbitol and galactitol, which accumulate in lens fibers, causing an increase of osmotic pressure leading to swelling and finally to changes in the contents of the lens resulting in opacification of the lens fibers and complete distortion of the lens (Varma and Kinoshita, 1976; Beyer-Mears and Fransworth, 1979; Bettelheim, 1985; Mitton and Trevithick, 1994). Heavy molecular weight lens protein aggregates have been demonstrated in aging normal and cataractous human lenses (Jedziniak *et al.*, 1975; Harding, 1980; Spector, 1985). Spector (1985) proposed possible causes of the unfolding and changing of proteins in cataractous lenses.

The various types of cataracts can be described on the basis of a biochemical change of the lens fiber proteins *or* on the basis of morphological changes. Biochemically, because under the influence of calcium ions lens fibers can swell, after which they degrade forming spherical bodies (Duncan and Bushell, 1976; Fagerholm, 1979). Morphologically, because biochemical changes can be observed as changes in the spatial arrangements of lens fibers (Creighton *et al.*, 1978, 1980; Ross *et al.*, 1983; Vrensen *et al.*, 1990; Vrensen, 1995).

Lens cells not only contain a high concentration of proteins, but also a rather high amount of cholesterol and even the lens gap junctions are characterized by a high content of cholesterol and may play an essential role in maintenance of the ultrastructural integrity of the lens, thereby preserving lens transparency (Alcala *et al*., 1983; Li *et al.*, 1985). Hence, formation of cataracts both in humans and in experimental animals may involve massive insolubilization of the soluble proteins of the lens, resulting in light scattering contributing to lens opacification (Cenedella and Fleshner, 1979; David *et al*., 1987). Damage to the lens cell membrane, followed by dissociation of specific proteins, has been suggested to be an early and perhaps initiating event in cataract formation (Bloemendal, 1977, 1991; De Vries *et al*., 1991; Vrensen *et al.*, 1992).

Two types of opacities have been distinguished: fiber based opacities, determined by the shape of the lens fiber, and non fiber based opacities. The first type shows a disruption of the lens fiber membrane and a disturbance of the cytoplasmic contents of the lens fiber, the cytoplasm having changed into a mass of globular elements. Each individual lens fiber represents a single tube with protoplasm, bordered by plasma membranes which extensively interdigitate with adjacent fibers by edge protrusions, grooves and ridges. The lens fibers are functionally linked to each other by gap junctions. It seems that an annealing process exists, to seal off the defective part of a lens fiber from the normal part and that a gap junctional mechanism exists, to separate a damaged fiber from normal adjacent fibers. In the deep cortex the transport of factors initiating fiber breakdown is limited due to the deviant architecture of the fiber-limiting membranes (Brown *et al.*, 1993). They have an extremely high cholesterol ratio, no intra-membrane particles and have a kind of "degenerated" gap junctions. The deep cortex lens fibers are impermeable to ions, nutrients and water, making them considerably less sensitive to cataractous changes (Duindam *et al.*, 1995).

In morphological studies by SEM and TEM, the presence of spherical bodies or vacuoles has been shown in cataractous material both in human and animal lenses, in the latter ones experimentally induced via X-ray irradiation (Ross *et al.*, 1983; Vrensen and Willekens, 1989; Vrensen *et al.*, 1990; Jongebloed *et al.*, 1992, 1993a,b; Brown *et al.*, 1993). The presence of these globular structures is characteristic for the degradation process occurring in the

lens cytoplasm during cataract formation. Although the presence of these structures has been reported earlier (Creighton *et al*., 1978), the emergence of globular structures penetrating the lens fiber membrane has so far not been shown in stereoscopic SEM images.

**Low voltage field emission-SEM and non-coating preparation**

In a field emission (FE)-SEM (SEM with a field emission cathode) micrographs can be taken at low accelerating voltage (approximately 2 kV) with a resolution almost equal to images obtained at 15-25 kV with a conventional SEM equipped with a W or $LaB_6$ cathode. The reason for this is the high brightness of the FE cathode, which produces a high density electron beam with a small diameter. The use of low voltage in FE-SEM has a number of advantages such as a more clear visualization of the surface structure of the sample, a significant reduction of charging and a considerable contrast enhancement in the image. This is the result of the decreasing number of secondary electrons from the deeper parts (bulk) of the specimen in favor of those coming from the surface area, leading to a better signal/noise ratio (Jongebloed *et al*., 1996).

Specimen preservation can be carried out either by chemical fixation followed by physical drying or by cryofixation followed by fracturing and etching (ice sublimation). Standard chemical fixation can be carried out by a prefixation with glutaraldehyde (GA) and a postfixation with osmium tetroxide ($OsO_4$). This must be followed by application of a thin conductive coating (approximately 1.5-2.0 nm) of Cr, Au/Pd or Pt via planar magnetron sputtering to avoid charging (Hayat, 1990). A postfixation by means of a non-coating procedure, such as the OTO(TO) or TAO technique considerably, improves both the preservation (fixation) of biological structures and the electrical conductivity. The OTO(TO) method stands for osmium-thiocarbo-hydrazide-osmium tetroxide (-thiocarbohydrazide-osmium tetroxide). Thiocarbohydrazide is a sulfur containing osmiophilic reagent which can reduce osmium tetroxide and react with certain aldehyde groups. Thiocarbohydrazide is very useful for structures that already have bound osmium, as is apparent from the sequence of steps in the procedure. The TAO method stands for tannic acid - arginine - osmium tetroxide. Tannic acid, or its main constituent galloyl glucose with its two phenolic groups bound to glycose, can bind in several ways to mucopolysaccharides, carbohydrates and metal ions, and is considered to be a supplemental fixative to glutaraldehyde. The superior preservation of the various constituents is the result of a high and a rather uniform uptake of osmium by the sample by the interaction of the ligands thiocarbohydrazide and tannic acid/arginine, respectively, thus obviating the need for an external conductive coating (Mizuhira and Futaesaku, 1974; Murakami, 1974; Simionescu and Simionescu, 1976; Murphy, 1978; Chaplin, 1985; Kalicharan *et al.,* 1993b). The use of osmium tetroxide alone or in combination with the given ligands seems at first sight not very appropriate, because of the high content of proteins making up the lens fiber. Cataractous material nevertheless reacts very well with galloyl glucose (the main constituent of tannic acid). The formed complex can bind several heavy metal ions such as osmium, ruthenium and lead, which contributes to an optimal fine structure preservation and conductivity for SEM observation.

**Stereoscopic imaging with SEM**

Why produce SEM stereo pairs of ophthalmic tissue for morphological investigations, when SEM images already give an impression of the 3-D structure of the sample? Large contrast differences can result in a false perspective, because dark often is associated with distance or areas hidden from the viewer, while bright is associated with areas closer to the viewer (Boyde, 1974, 1975). Large differences in image brightness often are the result of charging or the position of the given structure with respect to the secondary electron detector. The well known edge effect at sharp edges caused by secondary electrons emerging from both sides, often results in too bright edges as well. A stereo pair of images also can detect image changes due to vibration, vacuum faults, charging, or distortion of the specimen.

As a result of the high resolution of the FE-SEM, relative large working distances can be used, which increases the depth of field; in most cases a working distance of 12-24 mm was used. Moreover, due to the goniometer stage of the used FE-SEM, very accurate specimen displacements can be made in the X, Y and Z directions including the inclination. The correct movements and their readings are precision parameters necessary for a correct determination of depth and measurements in the third dimension as well as for a optimal 3-D appreciation.

A stereoscopic pair of images, produced by the combination of two images of exactly the same location and magnification, with only a difference in tilt angle of approximately 6-7°, gives the spatial relations of the structures in the specimen in a good perspective (Helmcke, 1955; Catto and Smith, 1972; Boyde, 1974, 1975).

**Aim of the study**

The aim of the study was to visualize, in stereoscopic images with FE-SEM in combination with the application of non-coating post fixation, the penetration of the lens fiber membrane in cataract lenses by globular structures for a better understanding of the degeneration process of the lens fiber.

## Materials and Methods

Eight human lenses with a posterior cortex cataract, obtained from patients in the age group of 65-80 years, were washed in 0.1 M sodium cacodylate buffer + 6.8 % sucrose for 30 seconds. Subsequently the lenses were cut into small blocks of approximately 2 x 2 x 2 mm containing cataractous areas and prefixed in 0.1 M sodium cacodylate buffered glutaraldehyde (2%) for 24 hrs at 4°C. The prefixed tissue blocks were sectioned (100-150 µm) with a vibratome and then rinsed (3x) for 5 min in 0.1 M sodium cacodylate buffer solution + 6.8 % sucrose. Subsequently the specimens were immersed in a mixture of 2% arginine-HCl, 2% sodium glutamate, 2% glycine and 2% sucrose in 0.1 M cacodylate buffer for 16 hrs at 20°C. After rinsing with buffer solution (3x), the specimens were immersed for 8 hrs in a mixture of 2% tannic acid and 2% guanidine-HCl in distilled water for 20°C. After washing (3x) in distilled water, the samples were fixed for 8 hrs in a 2% $OsO_4$ solution in water at 20°C and washed again (3x) in distilled water (Jongebloed *et al*., 1993b; Jongebloed and Kalicharan, 1994). After rinsing, the samples were dehydrated via an ethanol series up to 100 % ethanol and subsequently critical point dried from liquid $CO_2$. All specimens were examined in a JEOL (Tokyo, Japan) FEG-SEM, type 6301F, operated at 2 kV; working distance: 18-39 mm, beam current: $1.5 \times 10^{-11}$ A. Stereo images were prepared with a 6° tilt angle between the individual images of the stereo pair.

## Results

### Stereoscopic SEM images of healthy lens fibers (Figs. 1-4)

Stereoscopic images give a 3-dimensional view on the structure both of healthy and cataractous lens fibers, in particular on the complex structure of connections between lens fibers in one layer and between different layers of lens fibers. Figure 1 represents a fracture through a part of a healthy lens; the lens fibers can be seen from different directions as small elongated ribbons. In one layer they are interconnected via a kind of undulating system, which is typical for lens fibers in the posterior cortex or nuclear area. In the loosely bound part at the right side of the picture (A), the lens fibers are seen from a direction which is perpendicular to that of the main part of the picture (B). The lateral interdigitations or balls and socket connections of lens fibers aligned in radial cell column faces are not well visible because of the low magnification.

A fracture through a number of layers of healthy lens fibers from the cortical area, showing clearly their elongated shape, is shown in Figure 2. The interdigitation system, visible as a kind of zip-fastener, is partly locked and partly open showing the position of the lens fibers with respect to each other. The top part of the image (A) represents a similar view onto the lens fiber arrangement as seen in the right-hand side of Figure 1. The row of small knobs on top of the lens fiber parallel to the length of the ribbons, represents part of the connections with the lens fiber on top, which is, however, fractured away. The typical architecture of the lens fiber layer can be easily observed in this stereo pair of images.

Figures 3-4 represent a closer view of the ball and socket interdigitation system with flaps and imprints. The complex way of interlocking of the lens fibers in the different directions is clearly shown. The thickness of the individual lens fibers, as visible in the top part of the picture, is approximately 1-1.5 µm. The row of small, slightly charging, white knobs seen in Figure 3 represents the connections with the lens fiber on top, which has been fractured away. In Figure 4, a detail of the top area of Fig. 3, the connections with the lens fiber underneath can be seen just through the elliptical holes to the left and right neighbored by the flaps.

### Stereoscopic SEM images of cataractous lens fibers (Figs. 5-10)

Figure 5 shows a fracture through the cortical area of a cataractous lens. The lens fibers are visible in two directions. Large numbers of spherical structures are emerging from the space (A) between the layers (shells) of lens fibers, as can be seen in the bottom part of the picture. In the lateral face, the lens fibers are visible as elongated

*(Figure 1-4 on facing page)*

**Figure 1**. Stereo pair of fractured healthy lens fibers from the posterior cortex area. Note the elongated shape of the lens fibers and open as well as locked undulating (arrow) interdigitation system of lens fibers in areas (A) and (B). Bar = 10 µm.

**Figure 2**. Stereo pair of another fracture through compact and healthy lens fibers, note unlocked inter-digitation system in area (A) and typical knob-like expansions (arrow) at the lens fiber edge representing the connection with the lens fiber atop, but broken away. Bar = 10 µm.

**Figure 3**. Stereo pair of detail of fracture through lens fibers, note the ball and socket connections of the interdigitation system with flaps (arrow) and imprints (arrowhead). Note limited thickness of the lens fibers visible at (A). Bar = 1 µm.

**Figure 4**. Stereo pair of detail of interdigitation system of Fig. 3, note pin-hole (arrow) construction in three dimensions, comparable with those of Fig. 2. Bar = 1 µm.

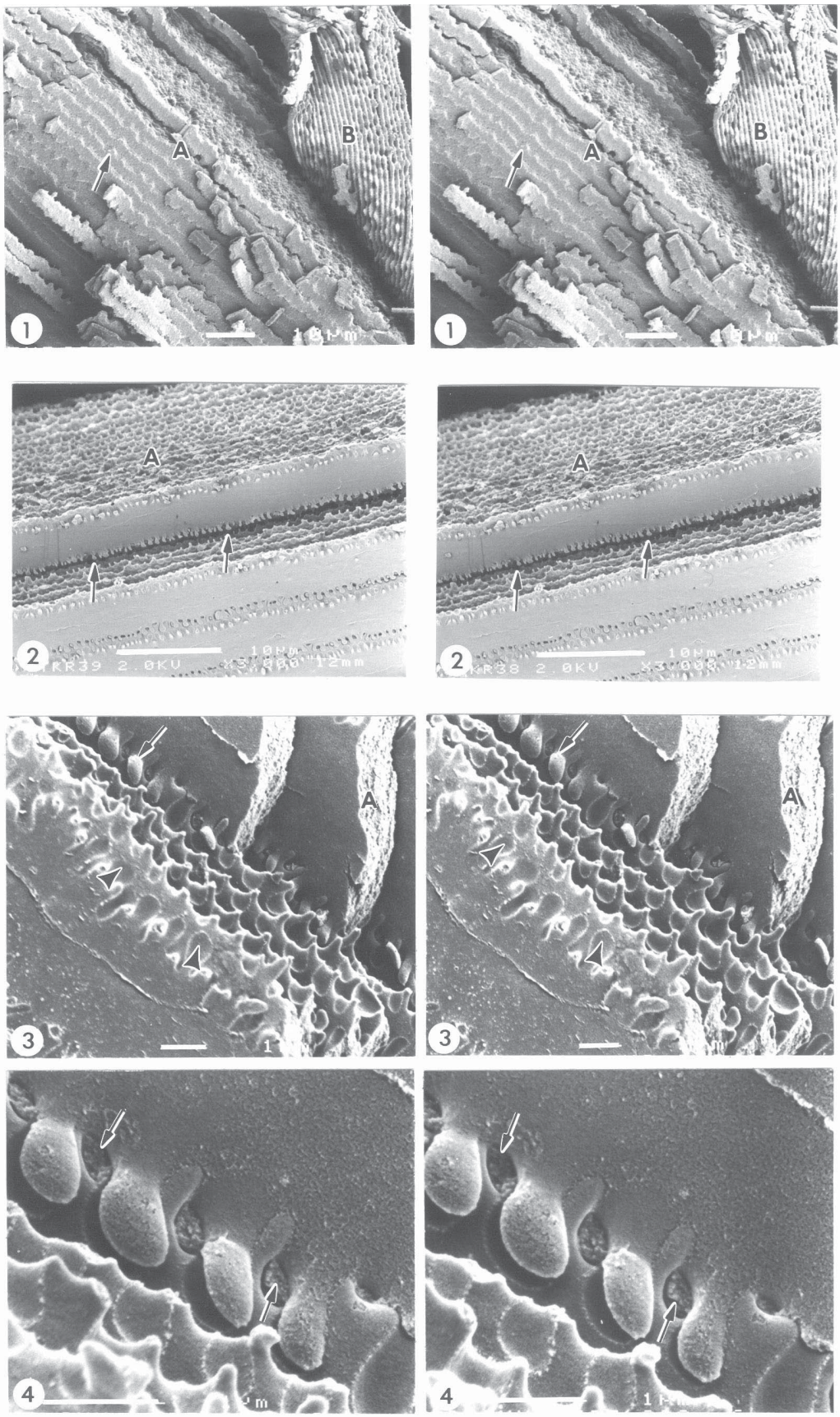
A
B
1
A
B
1
A
2
A
2
A
3
A
3
4
4

ribbons, the magnification is too small to see whether the interdigitation system is still intact. Both balloon-like structures and more spherically shaped structures with a large variation in size, have penetrated the lens fiber membrane and appear at the fracture surface.

A detail of area (A) of Figure 5 is shown in Figure 6, with emerging globular structures in between the different layers of lens fibers. From this image it is evident that the lens fiber membrane has been penetrated by these globules, so they emerge at the space between two adjacent lens fibers. These structures vary in size, some of them have a balloon-like appearance, suggesting that they have penetrated the lens fiber membrane under pressure.

Figure 7 shows a similar process. The shape of the globules is not always spherical, it seems that by penetrating the membrane the shape becomes more elliptical or balloon-like, or sometimes angular, indicating that these forms are dependent of the available space inside the cytoplasm. In the top part of the image, the membrane penetration can be clearly observed. The degradation process can be better seen in Figure 8. It seems that a considerable part of the lens fiber contents consists of spherical bodies and that only a kind of skeleton is remaining. Part of the globular structures is covered with which appears to be fragments of lens fiber membranes in different shapes, such as ring-shaped and rosette-like fragments or lamellae, visible on top of those globular structures.

Figures 9-10 show the penetration of the globules through the lens fiber membrane in more detail. Spherical bodies of varying diameter (approximately 1-6 μm) find their way through the already porous membrane. The granular appearance of the lens fiber membrane is quite obvious. Particularly from the onion-like peeled-off lamellae of the lens fiber membrane it is obvious that those fragments have a granular appearance particularly at the outside. Almost no substructure is seen at the globular wall, sometimes only fragments of the lens fiber membrane are attached. Some of these structures show light indentations, indicating that they possibly were formed under pressure inside the cytoplasm of the lens cell and are made of soft material easy to be shaped by pressure of bordering structures.

## Discussion

### Preparation and microscopical parameters

One of the prerequisites for an adequate observation of (cataractous) lens fibers is an excellent pre- and postfixation of the lens tissue. Inadequate or a delayed fixation of lenses can produce intercellular swelling, myelin figures and interrupted plasma membranes (Rafferty, 1984). Therefore fixation of lens tissue immediately after explant of the lens avoids serious post-mortem changes, such as membrane rupture or lysis. The use of conventional fixation techniques requires the application of a conductive coating, which can cause artefacts certainly with gold after diode sputtering, already visible at medium magnification with FE-SEM (Stokroos *et al.*, 1995).

From earlier publications (Jongebloed *et al.*, 1991, 1993a,b; Kalicharan, 1993a), it was already obvious that non-coating preparation techniques can give optimal preservation and conductivity of biological material, such as lens tissue. Postfixation of biological tissue with the OTO(TO) or TAO method, respectively, is a reproducible way of preserving delicate structures. When carried out according to the microwave oven procedure, it moreover is a very fast method (Jongebloed and Kalicharan, 1994; Peschar *et al.* , 1995). Non-coating ligands such as thiocarbohydrazide and tannic acid/-arginine enhance secondary electron emission, as result of an increased binding of osmium necessary for a superior image quality (Murakami, 1974; Simionescu and Simionescu, 1976; Murphy; 1978; Chaplin, 1985).

Thiocarbohydrazide is a sulfur containing osmiophilic reagent that has been known for years, and is employed for the detection of PAS-positive compounds often in combination with periodic acid. The vicinal hydroxyl or amino groups of the PAS-positive substances are oxidized to release aldehyde groups which can reduce osmium tetroxide. The reagents were introduced for the localization of polysaccharides (e.g., glycogen), mucopolysaccharides and glycoproteins (e.g., mucin) and for enhancing the contrast of lipid components. In the specimen preparation for (FE)-SEM, thiocarbohydrazide can easily bind to structures that already have bound osmium via one of the two $NH_2$ or SH groups, respectively, and in this way enhance the binding of osmium by the structures. This higher uptake of osmium has two advantages: improvement of the preservation and enhancement of the conductivity of the sample.

Tannic acid or galloyl glucose, the main constituent of tannic acid, contains two phenolic groups bound to glucose. The complex is hydrolyzable and potentially capable of multiple interactions with carbohydrates such as hyaluronic acid, glycoproteins, arginine, lysine and collagen. It can in fact react with carboxyl, hydroxyl and sulfonic groups of amino acids and facilitates the binding with lead, uranyl, iron and osmium. Galloyl glycose is the most effective with non osmicated structures. The uptake of those heavy metal ions enhances both the preservation and conductivity, which is of utmost importance for high resolution FE-SEM. Due to the chemical alterations inside the lens cell during cataractogenesis products (molecular complexes) are formed, which are highly conducive to galloyl glucose complex formation.

On the other hand, the high brightness cathode of the FE-SEM can produce high resolution images at *low*

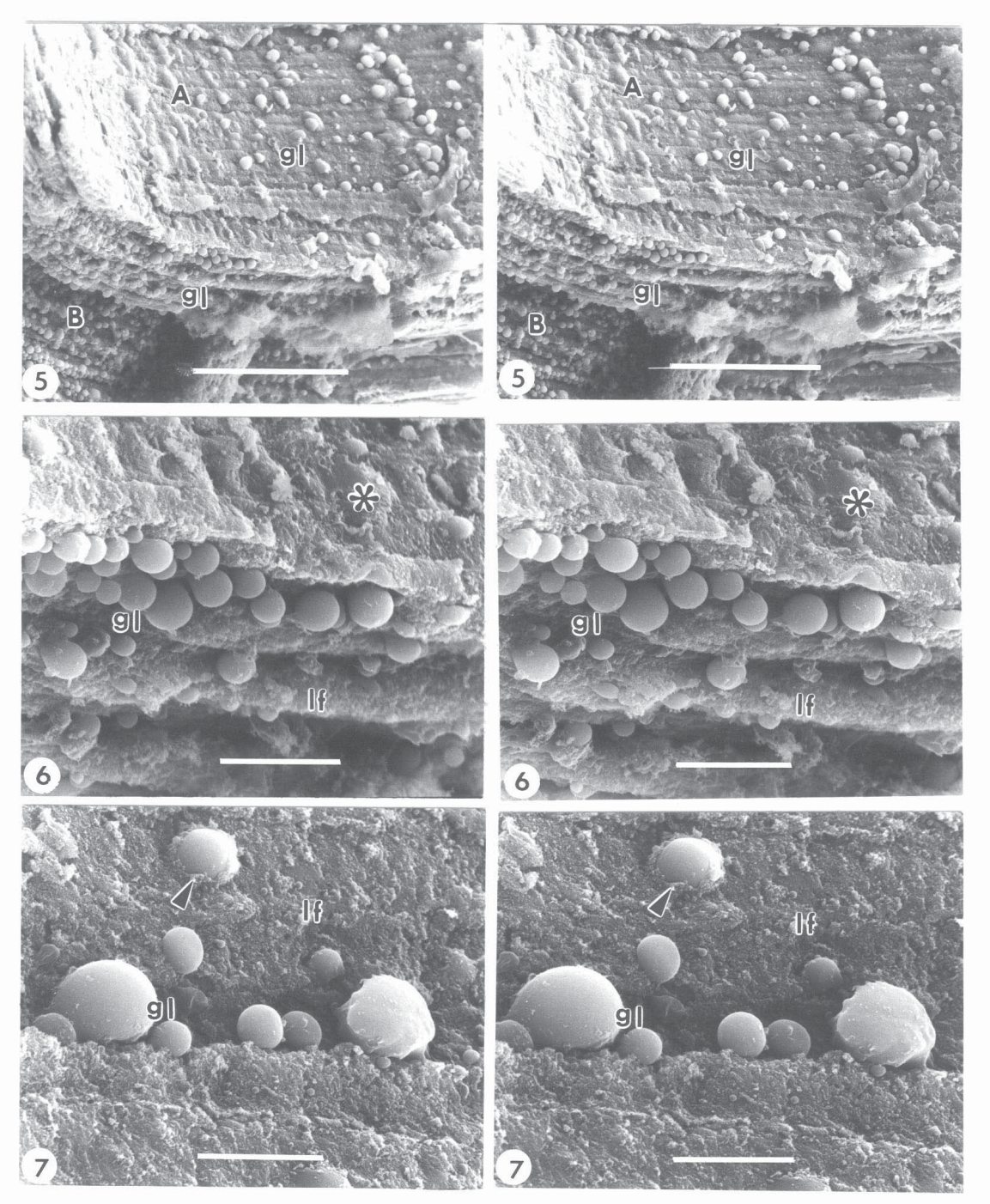


**Figure 5**. Stereo pair of fractured cortical section of a cataractous lens in top (A) and side view (B) with globules (gl) appearing in the intracellular space. Bar = 10 μm.

**Figure 6**. Stereo pair with detail of area B of Fig. 5, showing several layers of lens fibers (lf) in between which globules (gl) appear. The area indicated with * showing the lens fibers in lateral view is comparable with part of area A of Fig. 5. Bar = 5 μm.

**Figure 7**. SEM: stereo pair of a detail of cataractous lens fibers in top view with globular bodies (gl) of various shape and size emerging at the porous membrane of a lens fiber (lf), particularly noticeable at the site indicated with (s). Bar = 5 μm.

accelerating voltages, showing information of the sample surface in particular. A combination of low voltage FE-SEM and a non-coating preparation is quite appropriate for biological tissue, because then the secondary electrons are mainly generated in the superficial part of the specimen. It is quite obvious that the complex structure of the interdigitation system of lens fibers and the emerging of spherical bodies from the lens fiber membrane can be better understood from stereoscopic images (Kuszak *et al.*, 1988), than from single SEM and TEM images, the latter obtained from serial sections.

**Membrane changes**

Membrane rupture can occur as result of swelling; its occurrence and the presence of liquid-containing vacuoles and multilamellar bodies, the latter ones restricted to the superficial equatorial cortex, can be considered as age-related structural alterations of the lens fibers (Vrensen *et al.*, 1990). Membrane rupture and those vacuoles are the morphological support of the view that oxidative stress leads to destabilization and disintegration of membranes, resulting in disturbance of the water balance of the lens fiber; this is based on biochemical evidence. The vacuoles are mainly found in the superficial regions of the equatorial cortex, as shown by the absence of grooves and ridges at the lens fibers. After differentiation, lens fibers appear as long tubes filled with proteins surrounded by membranes studded with protrusions, grooves and ridges and ball and sockets as is visible in SEM and TEM images. From ultrathin sections studied by TEM it is obvious that lens fibers contain simple vacuoles with loosely or densely packed osmiophilic material and generally surrounded by a single or double membrane. Conglomerates of small electron dense condensations surrounded by a number of membrane-bound cytoplasmic elements suggest that they are in a stage of enwrapping the dense elements (Vrensen *et al.*, 1990). In TEM images often large numbers of small vacuoles are seen, individually enclosed by a membrane, not agglomerated to a large vacuole, but forming a extended field of vacuoles close to the limiting membrane of the lens fiber. These vacuoles are only partly filled with mostly non-osmiophilic material. The deterioration of the cell membrane is visible in the SEM as a porosity of that membrane and the fact that balloon-like protrusions can be observed, which take part of the membrane with them. It has been demonstrated that the degradation process of the lens fibers at the outside starts with deterioration of the lens fiber membrane, the sturdy appearance of the membrane is lost, folds and small pores in the membrane become obvious (Bloemendal, 1977; Eshaghian and Streeten, 1980; Anderson and Shearer, 1992; Costello *et al.*, 1992; Al-Ghoul and Costello, 1993).

Ross *et al.* (1983) found holes in the lens fiber membrane in rat eyes after ionizing radiation, while Worgul *et al*. (1980) demonstrated such holes after heavy particle radiation; both groups performed their experiments in *in vitro* systems. Vitamin E should decrease the damage caused by radiation, because of its free radical scavenging ability (McKay and King, 1980; Halliwell and Gutteridge, 1995). However, it is possible that the normal defense mechanism of a high level of antioxidant present to protect the lens and lens mem-branes *in vivo* is not available *in vitro*. In the cataract situation the defense mechanism may be hampered or not available anymore, leading to degradation of the membrane. The presence of glutathione could be another defense mechanism (Von Salmann and Munoz, 1952).

**Figure 8**. Stereo pair of cataractous lens fibers consisting of mainly globular material (gl), some of them covered with remnants in different shape and size of lens fiber membrane (*). Bar = 10 μm.

**Figure 9**. Stereo pair of emerging globules (gl), particularly at sites marked by (↔); some of these sites have indentations (*). Note the rather granular remnants (cross) of the lens fiber membrane at their top surface. Bar = 1 μm.

**Figure 10**. Stereo pair of higher magnification of some globules (gl), note shell-like remnants of the plasma membrane (pm) with a granular top surface with at left part of a lens fiber (lf). Bar = 1 μm.

**Globular structures**

Creighton *et al.* (1978) found in senile and diabetic posterior cortical subcapsular cataracts a zone in which the normal pattern of interdigitating cortical fibers had been disturbed. From the inner surface of the capsule downwards they found several layers: a spongy layer, a fibrous layer, a layer with globular degeneration of surfaces of lens fiber cells, lens cells with a blebbing surface with penetrating globules and cytoplasm con-taining fibrous material and cavities filled with globules, followed by normal lens cells containing globular bodies in spherical cavities. They indicated that lens fiber degeneration starts as formation of globules, which can have different appearances with respect to their outer surface. Sometimes it is spaghetti-like, while in other cases it is rather smooth only showing at high magnification a surface texture which possibly is the result of pebbled processes. The interpretation of these textured surfaces is somewhat difficult, because those images have been made at relative high kV, necessary to obtain optimal resolution and with rather thick Au-coatings (30-40 nm), to avoid charging. Au nuclei in these thick coatings easily agglomerate, producing an artefactual surface or decoration effect (Stokroos *et al.*, 1995).

It has also been suggested that extracellular globules represent fragments of cortical cells which appear rounded

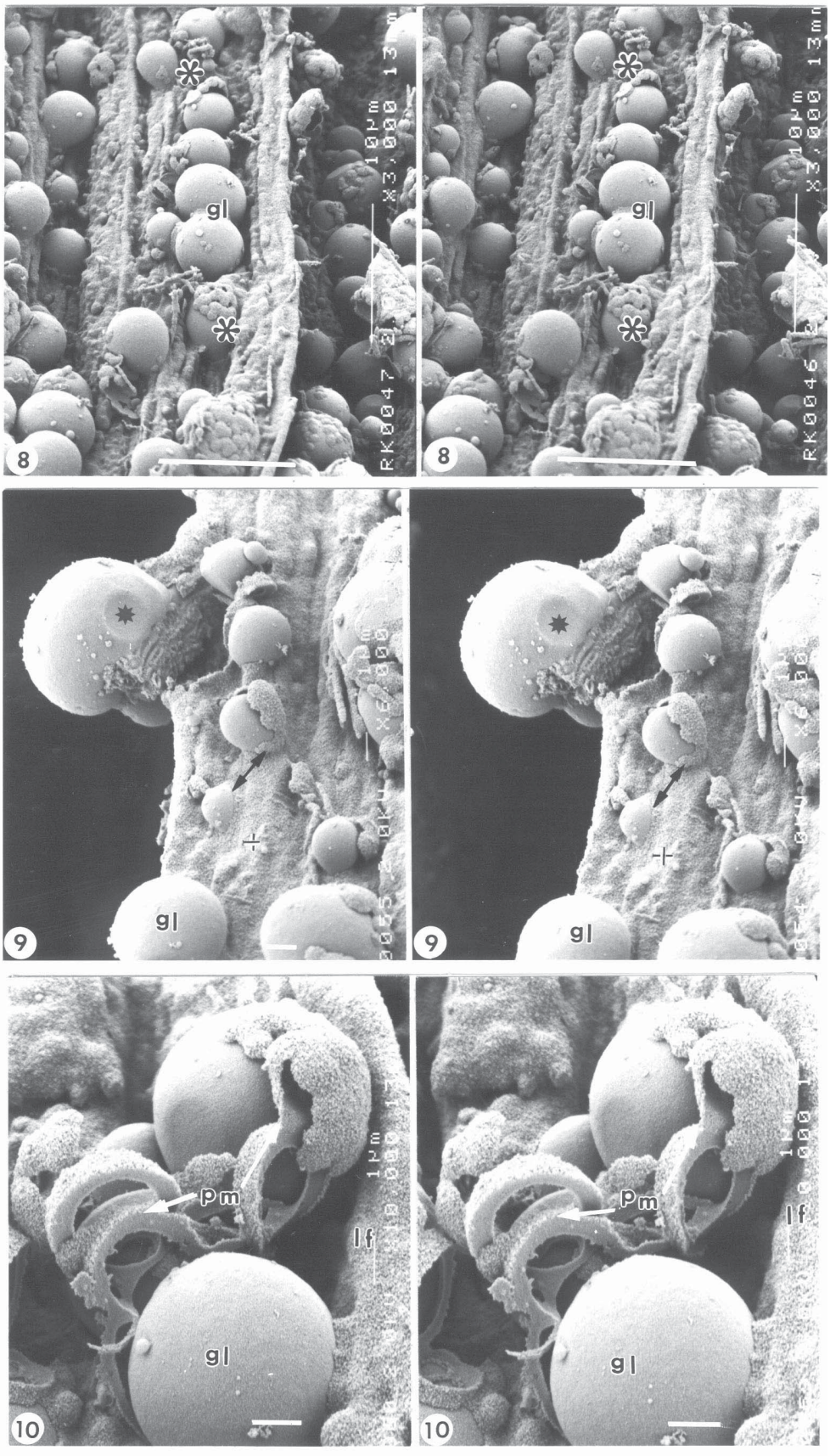
8
gl
8
gl
9
gl
9
gl
10
Pm
lf
gl
10
Pm
lf
gl

as result of increased liquidity of the cytoplasm. Creighton *et al*. (1978), suggest that subsurface actin micro-filaments of the cell fragment possibly by a kind of herniation and pass into *extracellular* globules formed when the cell cytoplasm produces large blebs at the cell surface. The small globular bodies found in normal old midzone lens fibers originate from intruding processes of an adjacent lens fiber. The intracellular globules appear to be excreted by the cells. Extracellular and intracellular globules contain γ-crystallites (Creighton *et al.*, 1978).

The FE-SEM images of cross fractures through the lens fiber suggest that at least part of the globular structures in the cataractous lens fiber are almost empty, filled with a fluffy content without contrast (not osmio-philic) or filled with viscous matter. The stereoscopic images give the impression that these (water) vacuoles penetrate the porous lens fiber membrane like a balloon. Some of the images show a tail-like extension at the balloon still connected with the lens fiber membrane. This type of penetration of a cell wall is also known from edemic processes in corneal endothelial cells (Jongebloed *et al*., 1987).

In the low kV FE-SEM images of the lens fiber membrane with penetrating spherical bodies, granular material was visible at the top of the emerging spherical body. The granular material seen at the outer surface of the lens fiber membrane in the SEM images is in good agreement with the images seen in the TEM, where often a thin layer of almost structureless material is found on top of the membrane structure. This granu-larity probably is an indication of a changing chemical constitution. The fact that remnants of the lens fiber membrane sometimes appear to have an onion ring-like shape, could be explained by the fact that the spherical bodies possibly still expand while penetrating the lens fiber membrane, by absorbing viscous material from the cytoplasm. When the globule breaks through the membrane, part of that membrane is coming along with the globule.

Obviously, there is to some extent a scale difference between the processes involving the spherical structures seen in SEM images and those seen in TEM. The numerous globules as found in the TEM images vary between 0.2 and 0.4 μm for the small ones with a reasonable contrast and between 0.5 and 0.9 μm for the slightly larger ones with obviously lower contrast. The vacuoles are larger in diameter: they range from 1.5 to 2.5 μm, and are almost empty. Sometimes much larger vacuoles are found containing a large number of 0.2-0.4 μm sized globules. The spherical bodies found in the SEM images most of the time are in the 1-3 μm size range (with exceptions up to 6 μm. The 1-3 μm size range is comparable with the vacuole-like structures (1.5-2.5 μm) seen in TEM images. The occurrence of spherical bodies at the porous membrane of the lens fibers as seen in the (stereoscopic) cataractous lens fibers is in good agreement with the images produced of TEM ultrathin sections. Numerous spherical bodies of approximately the same size are formed inside the cytoplasm and are moving towards the cell border with preference for the interdigitation area.

The cataractogenic processes can also lead to birefringent lenticular bodies, which have a crystallized ultrastructural globular appearance of approximately 10 μm in diameter, visible with the light microscope (Vrensen *et al.*, 1994). Some of the spherical bodies seen in the SEM images are damaged, they appear fractured and devoid of content (at least devoid of a dense or contrast-producing content). This is in agreement with the images of the vacuoles in the TEM. The average globular diameter is between 0.2 and 0.4 μm. Possibly, the small globules will eventually merge into larger ones (vacuole-like) and escape from the cyto-plasm. In TEM images sometimes small globules are seen with rather high contrast, apparently formed by inward folding of the membrane at the interdigitation area. If the globules grow at the expense of other globules their contents become less dense and lose contrast.

From the indentations (partly flat surface) on some of the spherical bodies, it can be concluded that the spheres have been formed at some pressure, which supports the notion that the spheres are formed by expansion from smaller ones. These indentations are also found in secondary cataract material obtained from ECCE (Extra Capsular Cataract Extraction) patients (Kalicharan *et al*., 1993a).

## Conclusions

1. The stereoscopic images of cataractous lens fibers clearly show the penetration of more or less globular structures through the cell membrane, which is indica-tive for a certain state of degeneration. This can also be concluded from the remnants of the cell membrane (often having the shape of an onion ring or rosette), clinging to these structures.

2. The shape and size of the penetrating bodies, varying from spherical to the shape of a football (elliptical), and the presence of indentations on their surface indicate that they are formed under pressure inside the cytoplasm of the lens cell.

3. As a result of the loss of connections between lens fibers in overlying layers, the globular structures can escape into the intracellular space and become visible in cross-fractures through the cataractous areas.

4. The use of non-coating techniques in combination with low voltage FE-SEM considerably facilitates ob-taining detailed information on the degrading lens fiber membrane.

## References


Alcala J, Katar M, Maisel H (1983) Lipid composition of chick lens fibre cell gap junctions. Curr Eye Res **2**: 569-578.

Al-Ghoul KJ, Costello MJ (1993) Morphological changes in human nuclear cataracts of late-onset diabetics. Exp Eye Res **57**: 469-486.

Anderson RS, Shearer TS (1992) Selenite nuclear cataractogenesis: a scanning electron microscopic study. Current Eye Res **11**: 1147-1160.

Bettelheim A (1985). Physical basis of lens transparency. In: The Ocular Lens Structure, Function and Pathology. Meisel H (ed)., Marcel Dekker, New York, pp. 265-300.

Beyer-Mears A, Farnsworth PN (1979) Diminished sugar cataractogenesis by quercetin. Exp Eye Res **28**: 709-716.

Bloemendal H (1977) The vertebrate eye lens. Science **197**: 127-138.

Bloemendal H (1991) Disorganization of membranes and abnormal intermediate filament assembly lead to cataract. Invest Ophthalmol Vis Sci **32**: 445-455.

Boyde A (1974) A stereo plotting device for SEM micrographs and real time 3-D system for SEM. Scanning Electron Microsc 1974: 93-100.

Boyde A (1975) Measurement of specimen height difference and beam tilt angle in anaglyph real-time stereo TV SEM system. Scanning Electron Microsc 1975: 189-198.

Brown NP, Harris ML, Shun-Shin GA, Vrensen GFJM, Willekens B, Bron AJ (1993) Is cortical spoke cataract due to lens fibre breaks? The relationship between fibre folds, fibre breaks, waterclefts and spoke cataracts. Eye **7**: 672-679.

Catto CD, Smith KCA (1972) A storage display system for the SEM. Scanning Electron Microsc 1972: 41-48.

Chaplin AJ (1985) Tannic acid in histology, a historical perspective. Stain Technol **60**: 219-231.

Cenedella RJ, Fleshner R (1992) Selective association of crystallins with lens "native" membrane during dynamic cataractogenesis. Curr Eye Res **11**: 801-815.

Costello MJ, Oliver TN, Cobo LM (1992). Cellular architecture in age related cataracts. Invest Ophthalmol Vis Sci **33**: 3209-3225.

Creighton MO, Trevithick JR, Mousa GY, Percy DH, McKinna AJ, Dyson C, Maisel H, Bradley R (1978) Globular bodies: a primary cause of the opacity in senile and diabetic posterior cortical subcapsular cataracts. Can J Ophthalmol **13**: 166-181.

Creighton MO, Steward-De Haan PJ, Ross WM, Sanwal M, Threvithick JR (1980) Modelling cortical cataractogenis. I. In vitro effects of glucose, sorbitol and fructose on intact rat lenses in medium 1999. Can J Ophthalmol **15**: 183-188.

David LL, Dickey BM, Shearer TR (1987) Origin of urea-soluble protein in the selenite cataract, the role of β-cristalline proteolysis and calpain II. Invest Ophthalmol Vis Sci **28**: 1148-1156.

De Vries ACJ, Vermeer MA, Hendriks ALAM, Bloemendal H, Cohen LH (1991) Bio-synthetic capacity of the human lens upon aging. Exp Eye Res **53**: 519-524.

Duindam HJ, Vrensen GFJM, Otto C, Puppels GJ, Grave J (1995) New approach to assess the cholesterol distribution in the eye lens: confocal Raman micro-spectroscopy and filipin cytochemistry. J Lipid Res **36**: 1139-1146.

Duke-Elder S (1969) Diseases of the lens, vitreous, glaucoma and hypotonia. In: System of Ophthalmology, vol XI. (C.V. Mosby, ed). H. Klimpton, London. pp 233-243.

Duncan G, Bushell AR (1976). The bovine lens as an ion exchanger. A comparison with ion levels in human cataractous lenses. Exp Eye Res **23**: 341-353.

Eshaghian J, Streeten BW (1980) Human posterior subcapsular cataract: an ultrastructural study of posteriorly migrating cells. Arch Ophthalmol **98**: 134-143.

Fagerholm P, Philipson BT (1977). Formation of after-cataract by regeneration of human and rabbit lens epithelium in tissue culture. Acta Ophthalmol **55**: 362-371.

Fagerholm PP (1979) The influence of calcium on lensfibres. Exp Eye Res **28**: 211-222.

Halliwell B, Gutteridge JMC (1985). Free Radicals in Biology and Medicine. Claredon Press, Oxford, pp 170-172.

Harding JJ (1980) Possible causes of the unfolding of proteins in cataract and a new hypothesis to explain the high prevalence of cataract in some countries. In: Aging of the Lens. Regnault F, Hockwin O, Courtois Y (eds). Elsevier, Amsterdam, pp. 71-80.

Hayat T (1990) Principles and Techniques of Electron Microscopy. Academic Press, London. pp 303-305.

Helmcke JG (1955) Theorie und Praxis der elektronenmikroskopischen Stereoaufnahmen. III: Methoden mit Tiefmessung elektronenmikroskopischer Objekte und Forderungen an ein photogrammetrisches Ausmessgerät (Theory and practice of electron microscopic stereo images. III: Methods with depth measurements on electron microscopic objects and requirements for a photogrammetric measuring equipment). Optik **12**: 253-273.

Hogan MJ, Alvarado JA, Weddell J (1971) Chapter 12. Lens In: Histology of the Human Eye. Hogan MJ, Alvarado JH, Weddell J, eds). JB Saunders, New York. pp. 638-677.

Jedziniak J, Kinoshita JH, Yates EM, Benedek GB (1975) The concentration and localization of heavy weight aggregates in aging normal and cataractous human lenses. Exp Eye Res **20:** 367-369.

Jongebloed WL, Dijk F, Worst JGF (1987) Descriptive anatomy of the aging process of the human cornea as visualized by SEM. Doc Ophthalmol **67**: 209-222.

Jongebloed WL, Kalicharan D, Los LI, Veen G van der, Worst JGF (1991) A combined scanning and transmission electron microscopic investigation of human (secondary) cataract material. Doc Ophthalmol **78**: 325-334.

Jongebloed WL, Kalicharan D, Los LI, Worst JGF (1992) Study of the substructure of the Morgagnian and Brunescens cataract with the TAO non coating technique; part I & II. Doc Ophthalmol **82**: 154-168.

Jongebloed WL, Kalicharan D, Worst JGF (1993a) The microscope in ophthalmological research. Microscopy and Analysis **25**: 5-7.

Jongebloed WL, Kalicharan D, Los LI, Worst JGF (1993b) The Morgagnian and Brunescens cataract morphology studied with SEM and TEM. Eur J Morphol **31**: 97-102.

Jongebloed WL, Dunnebier EA, Kalicharan D, Albers FWJ (1996) Visualization of the fine structure of stereocilia of the organ of Corti of the guinea pig by field emission gun scaning electron microscopy; variations in fixation technique and accelerating voltage. Scanning Microsc **10**: 147-164.

Jongebloed WL, Kalicharan D (1994) Tannic acid/ arginine/osmium tetroxide fixation of rat tissue by the microwave procedure. Beitr Elektronenmikroskop Direktabb Oberfl **27**: 243-252.

Kalicharan D, Jongebloed WL, Los LI, Worst JGF (1993a) Microorganisms found in secondary cataract material of ECCE patients, a study with SEM and TEM. Eur J Morph **31**: 103-106.

Kalicharan D, Jongebloed WL, Worst JGF (1993b). Lensfibre degeneration at cataract lenses. Doc Ophthalmol **85**: 77-86.

Kappelhof JP, Vrensen GFJM, de Jong PTVM, Pameyer JH, Willekens BLJC (1986) An ultrastructural study of Elschnig's pearls in the speudophakic eye. Am J Ophthalmol **101**: 58-69.

Kessel RG, Kardon RH (1979). Tissues and Organs: a Text Atlas of Scanning Electron Microscopy. Freeman, San Francisco. pp 95-100.

Kobayashi Y, Susuki T (1975). The aging lens, ultrastructural changes in cataract. In: Cataract and Abnormalities of the Lens. Bellows JG (ed). Grune and Stratton, New York. pp. 313-343.

Kuszak JR, Rae JL (1982). Scanning electron microscopy of the frog lens. Exp Eye Res **35**: 499-519.

Kuszak JR, Ennesser CA, Umlas J, Macsai-Kaplan MS, Weinstein RS (1988) The ultrastructure of fibre cells in primate lenses: A model for studying membrane senescence. J Ultrastruct Mol Struct **100**: 60-74.

Li L-K, So L, Spector A (1985) Membrane cholesterol and phospholipids in concentric sections of human lenses. J Lipid Res **26**: 600-609.

Maisel H, Harding CV, Alcala JR, Kuszak J, Bradley R (1981). The morphology of the lens. In: Molecular and Cellular Biology of the Eye Lens 1981. Bloemendal H (ed). Wiley and Sons, New York. pp 49-84.

McKay PB, King MM (1980) Vitamin E: Its role as a biological free radical scavenger and its relationship to the microsomal mixed-function oxidase system. In: Vitamin E: A Comprehensive Treatise. Machlin LE (ed.) Marcel Dekker, New York. pp. 289-317.

Mitton KP, Travithick JR (1994) High-performance liquid chromatography-electrochemical detection of antioxidants in vertebrate lens: glutathione, tocopherol, and ascorbate. Methods Enzymol **233**: 523-539.

Mizuhira V, Futaesaku Y (1974) New fixation for biological membranes using tannic acids. Acta Histochem Cytochem **5**: 233-236.

Murakami T (1974) A revised method for non-coated SEM specimens. Arch Hist Jap **36**: 189-193.

Murphy JA (1978). Non-coating techniques to render biological specimens conductive. Scanning Electron Microsc 1978; III: 175-195.

Peschar M, Kalicharan D, Jongebloed WL, Van der Want JJL (1995) FEG-SEM of non-coating microwave postfixed rat lung. In: Proc Annual Meeting Dutch Society for Microscopy (Jaarboek NVvM 1995). Berendsen W (ed). Karstens Drukkers, Leiden, The Netherlands. pp 118-119.

Rafferty NS (1985).Lens morphology. In: The Ocular Lens. Maisel H (ed.). Marcel Dekker, New York. pp 1-60.

Ross WM, Creighton MO, Inch WR, Trevithick J (1983) Radiation cataract formation diminished by vitamin E in rat lenses in vitro. Exp Eye Res **36**: 645-653.

Simionescu N, Simionescu M (1976) Gallolyl glucoses of low molecular weight as mordants in electronmicroscopy (I & II). J Cell Biol **70**: 608-633.

Spector A (1985). Aspects of the biochemistry of cataract. In: The Ocular Lens. Maisel H (ed). Marcel Dekker, New York. pp 405-438.

Stokroos I, Kalicharan D, Jongebloed WL (1995) A comparative study of ultrathin coatings for high resolution FEG-SEM. Beitr Elektronenmikr Direktabb Oberfl **28**: 165-172. Varma SD, Kinoshita JH (1976) Inhibition of lens aldose reductase by flavonoids, their possible role in the prevention of diabetic cataracts. Bioch Pharmacol **25**: 2505-2513.

Von Sallmann VL, Munoz CM (1952). Further efforts to influence X-ray cataract by chemical agents. Trans Am Ophthalmol Soc **49**: 391-417.

Vrensen G, Willekens B (1989). Classification and prevalence of early senile lens opacities in human donor eyes. In: Risk Factors for Cataract Development. Sasaki A, Hockwin O, Leske MC (eds). Karger, Basel. Dev Ophthalmol

**17**: 181-187.

Vrensen G, Kappelhof J, Willekens B (1990) Morphology of the aging lens; Part II: Ultrastructure of clear lenses. Lens and Eye Toxicity Res **7**: 1-30.

Vrensen G, Van Marle J, Van Veen H, Willekens B (1992) Membrane architecture as function of lens fibre maturation: a freeze fracture and scanning electron microscopic study in the human lens. Exp Eye Res **54**: 443-446.

Vrensen GFJM, Willekens B, De Jong PTVM, Shun-Shin GA, Brown NP, Bron AJ (1994) Heterogeneneity in ultrastructure and elemental composition of perinuclear retrodots. Invest Ophthalmol Vis Sci **35**: 199-206.

Vrensen GFJM (1995) Aging of the human eye lens, a morphological point of view. Comp Biochem Physiol **111A**: 519-531.

Willekens B, Vrensen G (1982) The three dimensional organization of lens fibres in the Rhesus monkey. Graeffe's Arch Clin Exp Ophthalmol **219**: 112-120.

Worgul BV, Merriam GR Jr, Low S, Rossi H (1980) Heavy charged particles and cataractogenesis. Invest Ophthalmol Vis Sci **19 suppl**: 87 (abstr.).

**Discussion with Reviewers**: All questions by reviewers were answered by changes in the text.